AI Enabled Wireless Communications with Real Channel Measurements: Channel Feedback

Article *in* Journal of Communications and Information Networks · September 2020

DOI: 10.23919/JCIN.2020.9200894

9 authors, including:

Guo Jiajia
Southeast University (China)

Chen Muhan
Southeast University (China)

AI Enabled Wireless Communications with Real Channel Measurements: Channel Feedback

Jiajia Guo, Xiangyi Li, Muhan Chen, Peiwen Jiang, Tingting Yang,
Weiming Duan, Haowen Wang, Shi Jin, Quan Yu

***Abstract*—Artificial intelligence (AI) has shown great potential in wireless communications. AI-empowered communication algorithms have beaten many traditional algorithms through simulations. However, the existing works just use the simulated datasets to train and test the algorithms, which can not represent the power of AI in practical communication systems. Therefore, Peng Cheng Laboratory holds an AI competition, National Artificial Intelligence Competition (NAIC): AI+wireless communications, in which one of the topics is AI-empowered channel feedback system design using practical measurements. In this paper, we give a baseline neural network design, QuanCsiNet, for this competition, and the details of the channel measurements. QuanCsiNet shows excellent performance on channel feedback and the complexity of the neural networks is also given.**

***Keywords*—NAIC, artificial intelligence, CSI feedback, channel measurements**

I. INTRODUCTION

Since the success achieved by artificial intelligence (AI) in ILSVRC-2012[1], deep learning (DL) has shown great potential in many areas, e.g., computer vision, natural language processing, and drug discovery[2]. In recent years, DL has also been a popular topic in communications[3,4] and beaten some state-of-the-art traditional communication algorithms in many domains, e.g., signal detection[5], channel estimation[6], channel prediction[7], code design[8], and channel state information (CSI) feedback[9]. Therefore, AI has been viewed as a revolutionary technology and one of the most eye-catching ideas in 6G[10]. However, the results of most existing works are based on numerical simulations and are not validated by practical communication systems. A serious concern is that the neural networks (NNs) may just learn the simulator. For example, in the DL-based CSI feedback, related works all use the dataset generated by COST 2100 channel model to train and test the NNs[11]. The COST 2100 channel model can not capture the channel feature perfectly and the NNs may just learn the channel model. Therefore, there is doubt whether the NNs trained by simulation datasets can represent the performance in practical communication systems.

To explore AI's practical performance in communication systems, Peng Cheng Laboratory (PCL) holds an AI competition, National Artificial Intelligence Competition (NAIC): AI+wireless communications[1]. One of the competition topics is DL-based CSI feedback system design using practical measurements. Its goal is to evaluate the practical performance of the DL-based CSI feedback in the measured channel, thereby showing the real potential of the AI-empowered communications and playing a role of the ImageNet in communications to attract more researchers in the communication and machine learning communities to make contributions to AI-empowered 6G communications.

In this paper, we first give a brief introduction to the background and related work of CSI feedback and propose the baseline system design, QuanCsiNet, which is based on the CsiNet architecture proposed in Ref. [9] and introduces the quantization module. Then, we introduce the channel measurement environment and setting. Finally, we evaluate the performance of the QuanCsiNet with different feedback overheads.

Manuscript received Aug. 03, 2020; accepted Sep. 05, 2020. The work was supported in part by National Key Research and Development Program 2018YFA0701602, National Science Foundation of China (NSFC) for Distinguished Young Scholars with Grant 61625106, the NSFC under Grant 61941104, and 2019B010136, Guangdong Province Basic and Applied Basic Research Foundation. The associate editor coordinating the review of this paper and approving it for publication was L. Bai.

J. J. Guo, X. Y. Li, M. H. Chen, P. W. Jiang, S. Jin. National Mobile Communications Research Laboratory, Southeast University, Nanjing 210096, China (e-mail: jiajiaguo@seu.edu.cn; 230208578@seu.edu.cn; 220190739@seu.edu.cn; peiwenjiang@seu.edu.cn; jinshi@seu.edu.cn).

T. T. Yang, W. M. Duan, Q. Yu. Peng Cheng Laboratory, Shenzhen 518000, China (e-mail: yangtingting820523@163.com; duanwm@pcl.ac.cn; quanyu@ieee.org).

H. W. Wang. Laboratory of Broadband Wireless Technology, Shanghai Institute of Microsystem and Information Technology, Chinese Academy of Sciences, Shanghai 201800, China (e-mail: haowen.wang@mail.sim.ac.cn).

[1]https://naic.pcl.ac.cn/frame/1

II. Background and Related Work

The massive multiple-input multiple-output (MIMO) system has been a key technology in the 5G cellular systems and also will be integral to 6G due to the need for higher spectral and energy efficiency[12,13]. In massive MIMO systems, the base stations (BSs) are equipped with a large number of antennas, thereby averaging out the effects of fading, thermal noise, and intra-cell interference[12]. However, these potential benefits are based on the assumption that the BS has obtained the instantaneous CSI and the accuracy of the CSI directly affects the performance of the massive MIMO systems. In time-division duplexing systems, the downlink CSI can be inferred from the uplink CSI utilizing the reciprocity between the downlink and uplink CSI. However, in frequency division duplexing systems, the downlink is difficult to achieve due to the weak reciprocity between the bi-directional channel. The user equipment (UE) has to estimate the downlink channel by the pilots sent by the BS first. Then, the estimated downlink CSI is fed back to the BS through the uplink. In MIMO systems, this strategy is feasible since the dimension of the CSI matrix is low due to the limited antennas at the BS.

However, in massive MIMO systems, this feedback leads to a large overhead and occupies many uplink bandwidth resources because the dimension of the CSI matrix is much higher due to the hundreds or even thousands of antennas at the BS. Compressive sensing, which exploits the sparsity of massive MIMO CSI in certain domain, is regarded as one promising technology to greatly reduce the feedback overhead[14]. In the compressive sensing based feedback methods, the compression process is greatly simplified but the reconstruction process often turns into an optimization problem, which is solved by iterative algorithms and demands great computing and time resources. Besides, the compressive sensing based methods only regard the CSI sparsity as prior information and ignore the environment characteristic[15]. Therefore, the compressive sensing based feedback strategy has not been applied to practical systems so far.

In recent years, DL-based image compression methods have beaten traditional algorithms easily. Inspired by this, the authors in Ref. [9] introduce DL to the CSI feedback problem and propose an autoencoder-based NN architecture, CsiNet. Simulation results on COST 2100 channel model show that the DL-based method outperforms the traditional algorithms by a large margin. Since then, the DL-based CSI feedback has been a popular research topic in wireless communications and many novel works have been done in this new area. The existing works can be divided into the following four categories.

• Designing novel NN architecture. This kind of works focuses on improving the feedback accuracy using the novel NN architecture, e.g., attention model[16], multiple-resolution convolutional architecture[17], large receptive field[15], depth-wise separable convolution[18], fully convolutional layer[19], non-local NN architecture[20], generative adversarial network[21], etc. According to Ref. [21], CisNet+ in Ref. [15] achieves the state-of-the-art performance in the indoor scenario with low complexity while DCGAN in Ref. [21] achieves the state-of-the-art one in the outdoor scenario with huge complexity.

• Bitstream generation. In practical systems, the UE has to feed back the CSI in the form of bitstreams rather than the float-point number. The non-uniform quantizer and an offset NN in Ref. [15] are introduced to DL-based CSI feedback to generate bitstreams and reduce quantization errors, respectively. The uniform quantizer is adopted in Refs. [22,23] and the gradient of the quantization operation is set to be 1. The performance comparison between 4-bit uniform quantization and binarization operation is also given in Ref. [22] . To further reduce the feedback overhead, entropy coding is introduced to DL-based CSI feedback in Ref. [24].

• Exploiting expert knowledge. The physical prior information of downlink CSI can be exploited to improve the feedback accuracy and reduce the overhead. The authors in Refs. [22,24] propose a distributed cooperative DL-based CSI feedback framework, which is based on the CSI magnitude correlation among nearby UEs. A long short-term memory architecture is adopted in Ref. [25] to extract the time correlation in the time-varying channel.

• Tackling practical deployment challenges. To meet the requirement of adaptative feedback, a multi-rate feedback framework is proposed in Ref. [15]. The effects of the imperfect feedback and the feedback security are considered in Ref. [26,27], respectively. In Ref. [28], we applying NN compression techniques, e.g., pruning and weight quantization, to the CsiNet+ in Ref. [15], thereby reducing the computational complexity.

As mentioned in section I, the works [9,15-28] all use the datasets generated by MATLAB to train and test the proposed methods, which can not well validate the power of the DL in the practical CSI feedback.

III. System Model

In this section, we will introduce the massive MIMO systems and the process of the DL-based CSI feedback, respectively.

A. Massive MIMO-OFDM System

Considering a typical MIMO system, the BS is equipped with $N_\mathrm{t} \gg 1$ transmit antennas and the UE is equipped with $N_\mathrm{r} \geqslant 1$ receiver antennas. The orthogonal frequency division multiplexing (OFDM) system is with $N_\mathrm{c} \gg 1$ subcarriers. The downlink received signal $y_{m,c}$ on the cth subcarrier at the mth

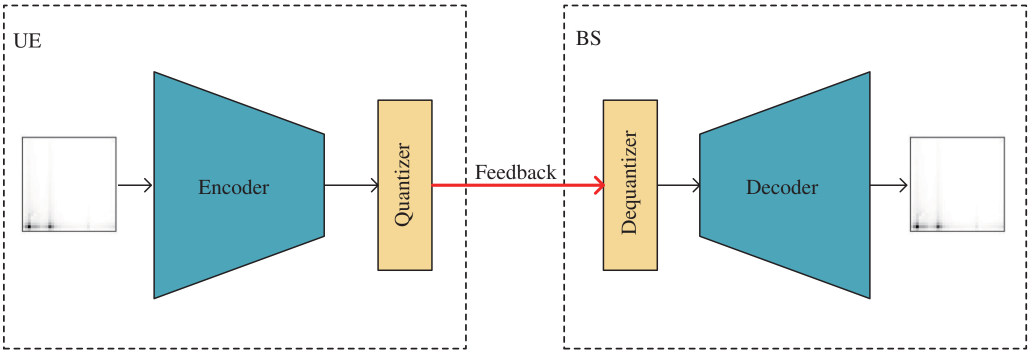

Figure 1 The bit-level DL-based CSI feedback framework

receiving antenna can be expressed as

$$y_{m,c} = \boldsymbol{h}_{m,c}^{\mathrm{H}} \boldsymbol{v}_c x_c + n_{m,c}, \tag{1}$$

where $\boldsymbol{h}_{m,c} \in \mathbb{C}^{N_\mathrm{t}\times 1}$ is the complex channel vector, $\boldsymbol{v}_c \in \mathbb{C}^{N_\mathrm{t}\times 1}$ represents the complex precoding vector, x_c is the complex data symbol transmitted in the downlink, and $n_{m,c}$ denotes the complex additive noise. The precoding vector $\boldsymbol{v} = \{\boldsymbol{v}_c : c = 1,\cdots,N_\mathrm{c}\}$ is selected at the BS, which seriously affects the performance of communication system. To achieve the precoding vector $\boldsymbol{v}_c$, the BS should know the accurate downlink CSI $\boldsymbol{H}_c = [\boldsymbol{h}_1,\cdots,\boldsymbol{h}_{N_\mathrm{r}}] \in \mathbb{C}_{N_\mathrm{t}\times N_\mathrm{r}}$. If the full downlink CSI $\boldsymbol{H}$ is fed back, the feedback dimension is $N_\mathrm{t}\times N_\mathrm{r}\times N_\mathrm{c}$. As mentioned in section I, in massive MIMO systems, the BS is equipped with substantial antennas, i.e., $N_\mathrm{t} \gg 1$, thereby making the dimension of full CSI extremely high. Therefore, feeding the full CSI back to the BS is unaffordable.

According to the spatial multipath channel model, the downlink channel $\boldsymbol{H}_c$ can be written as

$$\boldsymbol{H}_c = \sqrt{\frac{N_\mathrm{t}N_\mathrm{r}}{N_\mathrm{p}}} \sum_{l=1}^{N_\mathrm{p}} g_l \boldsymbol{a}_\mathrm{r}(\varphi_{\mathrm{r},l}) \boldsymbol{a}_\mathrm{t}(\varphi_{\mathrm{t},l}), \tag{2}$$

where N_p is the path number, g_l represents the complex gain of the lth path; $\boldsymbol{a}_\mathrm{t}(\cdot)$ and $\boldsymbol{a}_\mathrm{r}(\cdot)$ are the steering vector of the transmitter at the BS and the receiver at the UE, respectively; $\varphi_{\mathrm{t},l}$ and $\varphi_{\mathrm{r},l}$ denote the angle-of-departure and the angle-of-arrival, respectively.

B. DL-Based CSI Feedback Process

Fig. 1 shows the framework of the bit-level DL-based CSI feedback[2]. Here, we assume that the UE has obtained the perfect CSI, that is, ignoring channel estimation errors. For the existing DL-based CSI feedback, once the UE obtains the CSI $\boldsymbol{H}$, it first compresses the CSI matrix into a low-dimension vector with 32-bit floating-point numbers and then, the vector is discretized by a quantizer. This process can be expressed as

$$\boldsymbol{s} = \mathscr{Q}(f_\mathrm{en}(\boldsymbol{H},\Theta_\mathrm{en})), \tag{3}$$

[2]Since the entropy coding is lossless, we here ignore this part.

where $f_\mathrm{en}(\cdot)$ represents the compression operation, Θ_en is the NN weight, and $\mathscr{Q}$ denotes the quantization operation. The number of feedback bits N_bit is derived through the compression ratio $\gamma < 1$ and quantization bits B as

$$N_\mathrm{bit} = L\times\gamma\times B, \tag{4}$$

where L is the dimension of the full CSI. Once the BS receives the feedback from the uplink, it first dequantizes the feedback and then reconstructs the CSI using the NNs, which can be expressed as

$$\hat{\boldsymbol{H}} = f_\mathrm{de}(\mathscr{D}(\boldsymbol{s}),\Theta_\mathrm{de}), \tag{5}$$

where $f_\mathrm{de}(\cdot)$ represents the reconstruction operation, Θ_de is the corresponding NN weight, and $\mathscr{D}$ denotes the dequantization operation.

To evaluate the recovery performance of the framework we propose, normalized mean square error (NMSE) is introduced, which is defined as

$$\mathrm{NMSE} = \mathbb{E}\left\{\frac{\|\boldsymbol{H}-\hat{\boldsymbol{H}}\|_2^2}{\|\boldsymbol{H}\|_2^2}\right\}, \tag{6}$$

where $\|\cdot\|_2$ is the Euclidean norm.

IV. STRUCTURE OF QUANCSINET

In this section, we will introduce a specific network structure, i.e. QuanCsiNet, which compresses, quantizes, and reconstructs the downlink CSI.

Based on DL, we exploit the encoder and decoder structures via deploying a series of NN layers and training them to mimic the performance of encoder and decoder, i.e. $f_\mathrm{en}(\cdot)$ in (3) and $f_\mathrm{de}(\cdot)$ in (5), respectively. These NN layers are used for exploiting spatial local correlation by enforcing a local connectivity pattern among the neurons of adjacent layers.

We propose a DL model, named QuanCsiNet, which is specialized in dealing with CSI compression and feedback process. Based on a former DL work, CsiNet[9], QuanCsiNet adds quantization ($\mathscr{Q}$) and dequantization ($\mathscr{D}$) operations to further compress the feedback CSI, as well as making

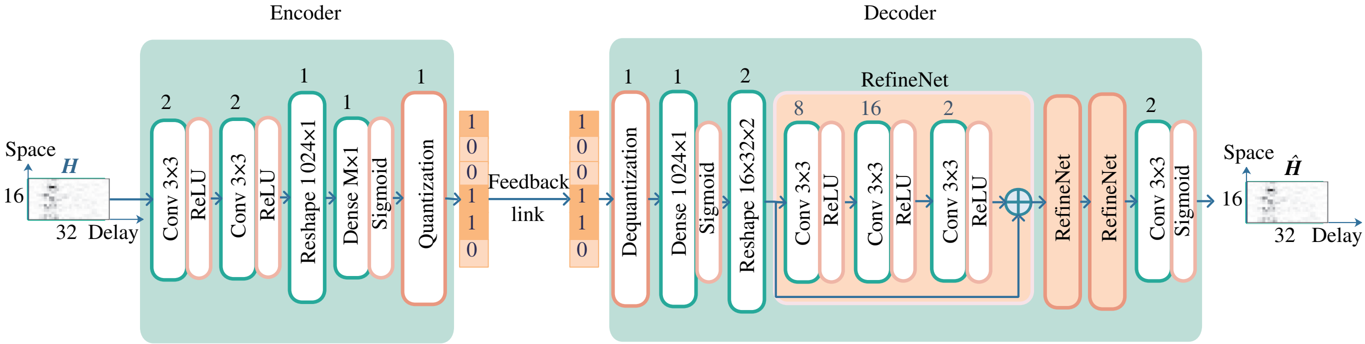

Figure 2 The structure of QuanCsiNet

some adjustment to better fit the new channel scenario. The overview of QuanCsiNet NN's structure is depicted in Fig. 2.

The input of the encoder is a $16\times32\times2$ matrix $\boldsymbol{H}$, where "2" means its real and imaginary parts and is first fed into two 3×3 convolution layers for a primary feature extraction, which is followed by activation "ReLU". Then, the two CSI feature maps are reshaped into an L-length vector for the next dense layer to output an M-length compressed code, i.e. $M = L\times\gamma\,(\gamma<1)$.

Notice that the feedback CSI signal is actually transmitted in the form of bitstream, and quantization operation is indispensable in communication systems. Here we apply uniform quantization with the quantization bits B. The output of the quantization layer is an N_{bit}-length ($N_{\text{bit}} = M\times B$) code in the form of bitstream, i.e. $\boldsymbol{s}$ in (3), where each element is either 0 or 1. Since this operation is differentiable, we set its gradient to be one[22]. Once the BS receives $\boldsymbol{s}$, it inputs $\boldsymbol{s}$ to the dequantization layer to transform back from bitstream form to "float32" numbers.

After dequantization, the M-length vector is first put into a dense layer to output an L-length vector and reshsaped into $16\times32\times2$-sized CSI feature maps as a rough reconstruction. Then, three RefineNet blocks[9] are applied to recover more detailed features. In each RefineNet block, three 3×3 convolutions are stacked together, which outputs 8/16/2 feature maps, respectively. An activation "ReLU" is followed with each of them. Moreover, a residual connection is built from the input to the output in each RefineNet block to avoid network degradation problem. At the end of the decoder, a 3×3 convolution is applied and an activation "Sigmoid" is used for normalizing the output values in [0,1].

QuanCsiNet is trained end-to-end by updating parameters in the procedure of minimizing the mean squared error loss function using the ADAM algorithm, which can be given as

$$L = \frac{1}{N}\sum_{i=1}^{N}\|f_{\text{AE}}(\boldsymbol{H}_i;\Theta_{\text{AE}}) - \boldsymbol{H}_i\|_2^2, \tag{7}$$

where $f_{\text{AE}}(\cdot)$ represents the QuanCsiNet and N denotes the total number of examples in the training data.

V. Experiment and Analysis

In this section, we first introduce the downlink channel measurements in office scenario. Then, we illustrate the training process in details and analyse the experimental results on this practical CSI dataset.

A. *Channel Measurements*

The wireless channel data are measured by PCL in the actual channel environment as shown in Fig. 3. The central frequency of the system is 3.5 GHz and the bandwidth is 100 MHz, equipped with $N_{\text{t}} = 4$ transmit antennas, $N_{\text{r}} = 4$ receiving antennas, and $N_{\text{c}} = 256$ subcarriers. The position of the transmitter is marked in Fig. 3, and the receiver moves along the trajectory of the red points at a speed of 1.5 m/s. The red points are the data collection positions of the receiver and the distance between the adjacent two red points is 1 m. The labeled point 1 and the labeled point 51 are 3 m and 5 m away from the transmitter, respectively. A total of 100 sets of data are tested. The starting point of each set is the corresponding point of the labeled value, and the ending point is the corresponding point of the next value, e.g., the 26th set of data is the data from point 26 to point 27 in Fig. 3.

The data collected by the receiving antennas are stored as channel components on each transceiver pair in the delay domain with a dimension of 256×1. The channel components of 16 transceiver pairs are stacked in the spatial-delay domain to form a complete channel matrix with a dimension of 256×16. Fig. 4 shows the processing flow of the measured channel data. After the channel data in the spatial-delay domain are obtained, we take the average peak noise as the measurements and set an appropriate threshold, and then eliminate the data with signal-to-noise ratio less than the threshold value, thus generating 320 000 samples. Due to the finiteness of the delay spread, we only retain the first 32 rows of the channel data in the delay domain to obtain a 32×16 truncated channel matrix.

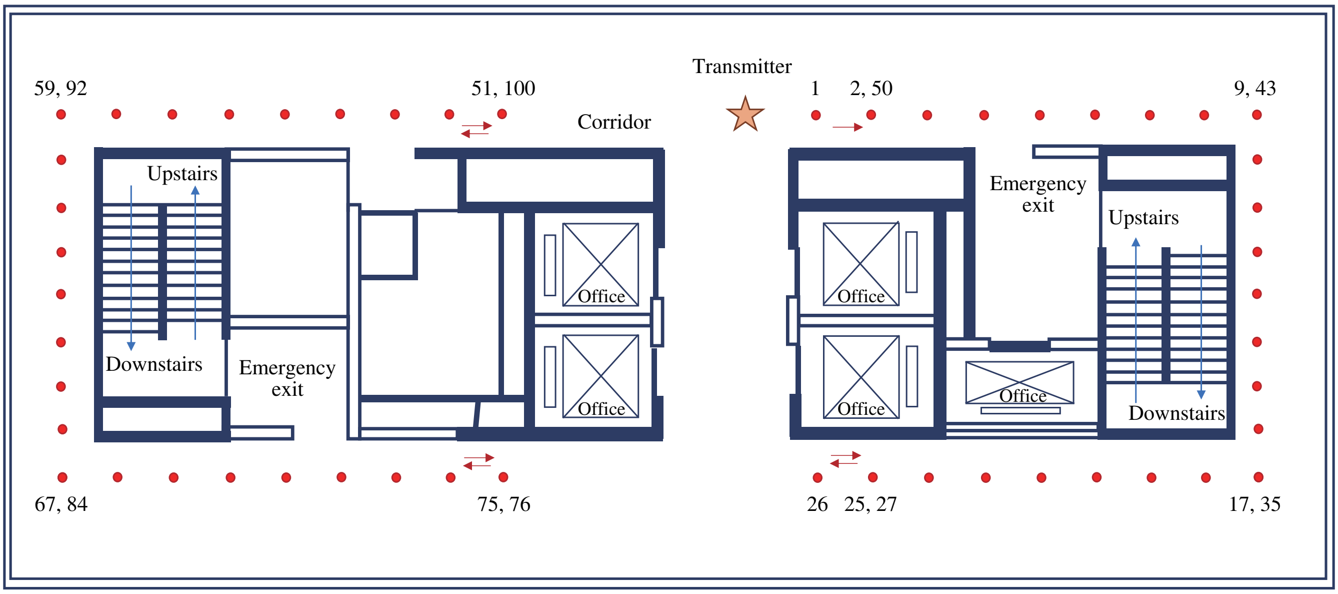

Figure 3 The schematic diagram of the measured channel scenario

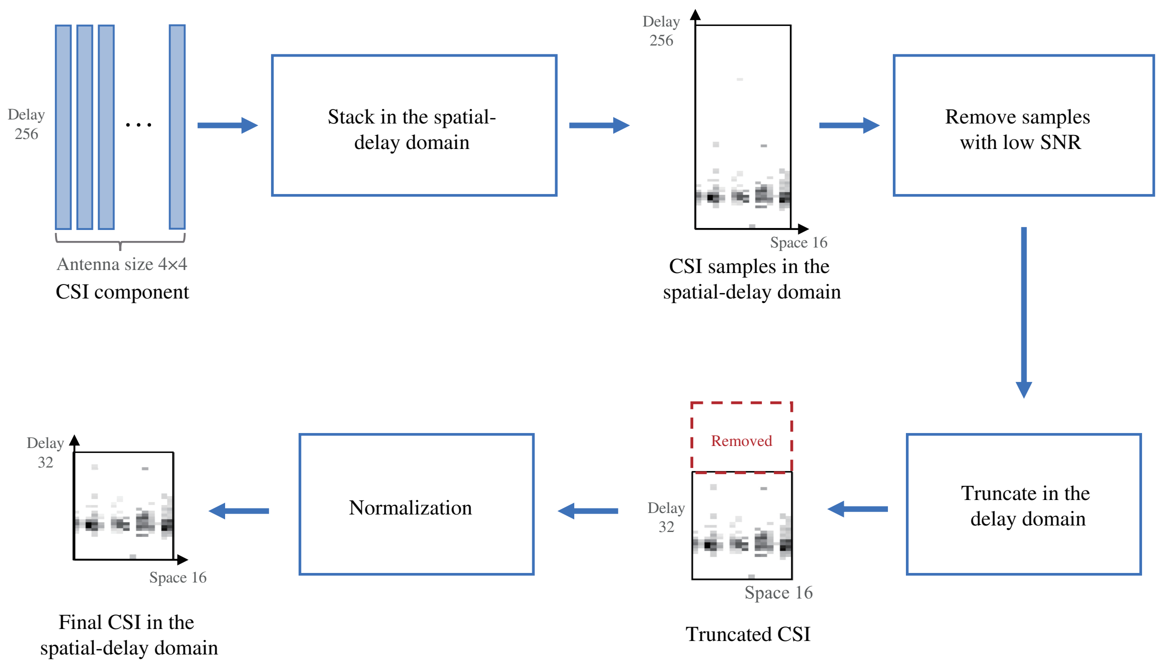

Figure 4 The flow chart of data processing for measured channel

Normalization is carried out for each sample to generate the final spatial-delay domain samples for the experiments. The training, validation and testing sets contain 300 000, 10 000 and 10 000 samples respectively.

B. Numeral Results

The batch size we use is 256 and the learning rate is set to 10^{-3} for the 1 000 epochs. Different quantization bits B are used to test the performance of QuanCsiNet and the NMSE results are shown in Tab. 1. When quantization bits B is fixed, NMSE performance is improved as the feedback bits

Table 1 NMSE (dB) of QuanCsiNet with different B

Feedback bits (N_{bit})	128 bits	256 bits	512 bits	1 024 bits
QuanCsiNet ($B=4$)	−5.058	−7.308	−10.442	−13.480
QuanCsiNet ($B=8$)	−2.670	−5.138	−7.266	−10.321
QuanCsiNet ($B=32$)	−0.751	−1.263	−2.612	−4.898

Table 2 The number of parameters and FLOPs of QuanCsiNet with different B

	Feedback bits (N_{bit})	128 bits	256 bits	512 bits	1 024 bits
Parameters	QuanCsiNet ($B=4$)	71 536	137 104	268 240	530 512
	QuanCsiNet ($B=8$)	38 752	71 536	137 104	268 240
	QuanCsiNet ($B=32$)	14 164	22 360	38 752	71 536
FLOPs	QuanCsiNet ($B=4$)	5.129 M	5.260 M	5.523 M	6.049 M
	QuanCsiNet ($B=8$)	5.064 M	5.129 M	5.260 M	5.523 M
	QuanCsiNet ($B=32$)	5.014 M	5.030 M	5.063 M	5.128 M

N_{bit} grows. On one hand, under the same N_{bit}, the network with small B outperforms that with large B. On the other hand, when the compressed dimension is fixed, the NMSE preformance of the network with small B is comparable to that of the network with large B, which indicates that QuanCsiNet compensates for the influence of quantization errors to some extent.

The model complexity analysis of QuanCsiNet with different B is depicted in Tab. 2, where the number of parameters and FLOPs stand for space and time complexity, respectively. Under different quantization bits B, the amount of parameters will largely increase when the feedback bits N_{bit} increases, while the amount of FLOPs remains nearly the same (FLOPs values between 5.0 M and 6.0 M). This is because feedback bits N_{bit} has a great effect on the amount of parameters, i.e., dense layers in encoder and decoder, which includes most parameters; while most FLOPs come from the convolution operations. Moreover, under the same N_{bit} situation, different Quantization schemes can be selected, and a larger B indicates a smaller model (smaller space complexity).

Combining with the analysis in Tab. 1 and Tab. 2, QuanCsiNet ($B=4$) achieves best performance on CSI reconstruction while paying the price of the highest model complexity. When deploying in practice, we should combine with the actual situation and balance the NN's performance and model complexity.

VI. Conclusion

In this paper, we introduce the NAIC AI+wireless channel feedback using practical measurements. To explore the practical power of AI in wireless communications, we train and test the bit-level DL-based CSI feedback NN, QuanCsiNet using the practical measurements. Experiment results show the excellent performance of the DL-based CSI feedback. We hope the results in this paper can encourage more researchers in communications to make contributions to AI-empowered communications.

References

[1] KRIZHEVSKY A, SUTSKEVER I, HINTON G E. ImageNet classification with deep convolutional neural networks[C]//Advances in Neural Information Processing Systems 25. New York: Curran Associates, Inc., 2012: 1097-1105.

[2] LECUN Y, BENGIO Y, HINTON G. Deep learning[J]. Nature, 2015, 521(7553): 436-444.

[3] WANG T Q, WEN C K, WANG H Q, et al. Deep learning for wireless physical layer: Opportunities and challenges[J]. China Communications, 2017, 14(11): 92-111.

[4] QIN Z J, YE H, LI G Y, et al. Deep learning in physical layer communications[J]. IEEE Wireless Communications, 2019, 26(2): 93-99.

[5] YE H, LI G Y, JUANG B H. Power of deep learning for channel estimation and signal detection in OFDM systems[J]. IEEE Wireless Communications Letters, 2018, 7(1): 114-117.

[6] SOLTANI M, POURAHMADI V, MIRZAEI A, et al. Deep learning-based channel estimation[J]. IEEE Communications Letters, 2019, 23(4): 652-655.

[7] YANG Y W, GAO F F, LI G Y, et al. Deep learning-based downlink channel prediction for FDD massive MIMO system[J]. IEEE Communications Letters, 2019, 23(11): 1994-1998.

[8] KIM H, JIANG Y H, KANNAN S, et al. Deepcode: Feedback codes via deep learning[C]//Advances in Neural Information Processing Systems 31. New York: Curran Associates, Inc., 2018: 9436-9446.

[9] WEN C K, SHIH W T, JIN S. Deep learning for massive MIMO CSI feedback[J]. IEEE Wireless Communications Letters, 2018, 7(5): 748-751.

[10] DANG S, AMIN O, SHIHADA B, et al. What should 6G be[J]. Nature Electronics, 2020, 3(1): 20-29.

[11] CHEN M H, GUO J J, LI X, et al. An overview of the CSI feedback based on deep learning for massive MIMO systems[J]. Chinese Journal on Internet of Things, 2020, 4(1): 33-44.

[12] MARZETTA T L. Noncooperative cellular wireless with unlimited numbers of base station antennas[J]. IEEE Transactions on Wireless Communications, 2010, 9(11): 3590-3600.

[13] SAAD W, BENNIS M, CHEN M. A vision of 6G wireless systems: Applications, trends, technologies, and open research problems[J]. IEEE Network, 2020, 34(3): 134-142.

[14] QIN Z J, FAN J C, LIU Y W, et al. Sparse representation for wireless communications: A compressive sensing approach[J]. IEEE Signal Processing Magazine, 2018, 35(3): 40-58.

[15] GUO J J, WEN C K, JIN S, et al. Convolutional neural network-based multiple-rate compressive sensing for massive MIMO CSI feedback: Design, simulation, and analysis[J]. IEEE Transactions on Wireless Communications, 2020, 19(4): 2827-2840.

[16] CAI Q Y, DONG C, NIU K. Attention model for massive MIMO CSI compression feedback and recovery[C]//Proceedings of 2019 IEEE

Wireless Communications and Networking Conference. Piscataway: IEEE Press, 2019: 1-5.

[17] LU Z L, WANG J T, SONG J. Multi-resolution CSI feedback with deep learning in massive MIMO system[C]//Proceedings of 2020 IEEE International Conference on Communications. Piscataway: IEEE Press, 2020: 1-6.

[18] LI X Y, WU H M. Spatio-temporal representation with deep neural recurrent network in MIMO CSI feedback[J]. IEEE Wireless Communications Letters, 2020, 9(5): 653-657.

[19] CAO Z, SHIH W T, GUO J J, et al. Lightweight convolutional neural networks for CSI feedback in massive MIMO[J]. arXiv:2005.00438, 2020.

[20] YU X T, LI X Y, WU H M, et al. DS-NLCsiNet: Exploiting non-local neural networks for massive MIMO CSI feedback[J]. IEEE Communications Letters, 2020.

[21] TOLBA B, ELSABROUTY M, ABDU-AGUYE M G, et al. Massive MIMO CSI feedback based on generative adversarial network[J]. IEEE Communications Letters, 2020.

[22] GUO J J, YANG X, WEN C K, et al. DL-based CSI feedback and cooperative recovery in massive MIMO[J]. arXiv:2003.03303, 2020.

[23] LU C, XU W, JIN S, et al. Bit-level optimized neural network for multi-antenna channel quantization[J]. IEEE Wireless Communications Letters, 2020, 9(1): 97-90.

[24] YANG Q Q, MASHHADI M B, GUNDUZ D. Distributed deep convolutional compression for massive MIMO CSI feedback[J]. arXiv:2003.04684, 2020.

[25] WANG T Q, WEN C K, JIN S, et al. Deep learning-based CSI feedback approach for time-varying massive MIMO channels[J]. IEEE Wireless Communications Letters, 2019, 8(2): 416-419.

[26] YE H Y, GAO F F, QIAN J, et al. Deep learning-based denoise network for CSI feedback in FDD massive MIMO systems[J]. IEEE Communications Letters, 2020, 24(8): 1742-1746.

[27] LIU Q, GUO J J, WEN C K, et al. Adversarial attack on DL-based massive MIMO CSI feedback[J]. Journal of Communications and Networks, 2020, 22(3): 230-235.

[28] GUO J J, WANG J H, WEN C K, et al. Compression and acceleration of neural networks for communications[J]. IEEE Wireless Communications, 2020, 27(4): 110-117.

About the Authors

Jiajia Guo received his B.S. degree from Nanjing University of Science and Technology, Nanjing, China, in 2016, and his M.S. degree from University of Science and Technology of China, Hefei, China, in 2019. He is currently working towards his Ph.D. degree in information and communications engineering, Southeast University, China. His research interests currently include deep learning, neural network compression, massive MIMO, and machine learning in communications.

Xiangyi Li was born in Beijing, China, in 1994. She received her B.S. degree from the School of Mathematics, Tianjin University, Tianjin, China, in 2017, and her M.S. degree from the Centre for Applied Mathematics, Tianjin University, in 2020. She is currently working towards her Ph.D. degree in information and communications engineering, Southeast University, China. Her main research focuses on deep learning application in wirless communication and massive MIMO systems.

Muhan Chen was born in Jiangsu, China, in 1997. She received her B.S. degree from the School of Information Science and Engineering, Southeast University, Nanjing, China, in 2019. She is currently working towards her M.S. degree with the School of Information Science and Engineering, Southeast University, Nanjing, China. Her research interests center around deep learning applications in wireless communication systems.

Peiwen Jiang received his B.S. degree from Southeast University, Nanjing, China in 2019. He is currently working towards his Ph.D. degree with the School of Information Science and Engineering, Southeast University. His research interests include deep learning based channel estimation and signal detection in communications.

Tingting Yang received her B.Sc. and Ph.D. degrees from Dalian Maritime University, China, in 2004 and 2010, respectively. She is currently a Research Professor at Peng Cheng Laboratory, China. Her research interests are in the areas of maritime wideband communication networks, AI-empowered wireless communications. She serves as the Associate Editor-in-Chief of the IET Communications, as well as the Advisory Editor for SpringerPlus.

Weiming Duan is now a Senior Engineer in Peng Cheng Laboratory. He received his M.S. degree in communication and information system from the University of Electronic Science and Technology of China (UESTC) in 1999. In the same year, he joined Huawei Wireless Research Department in Shanghai and has worked there for 20 years. He has worked on baseband algorithm for 3G/4G, advanced receiver for 4G, waveform concept research for 5G, and has also been deeply involved in low-level algorithm library optimization to speed up large-scale system simulation.

Haowen Wang is a Senior Engineer of Laboratory of Broadband Wireless Technology, Shanghai Institute of Microsystem and Information Technology, Chinese Academy of Sciences (SIMIT). He received his B.S. and M.S. degrees from EE department and College of Software of Fudan University. In SIMIT, Haowen is a leader of wireless technology R&D group. He has many years of experience in the test and verification for the new technologies of wireless communications. His job and research interests include RF data acquisition, channel measurement, verification and test solution.

Shi Jin [corresponding author] received his B.S. degree in communications engineering from Guilin University of Electronic Technology, Guilin, China, in 1996, his M.S. degree from Nanjing University of Posts and Telecommunications, Nanjing, China, in 2003, and his Ph.D. degree in information and communications engineering from Southeast University, Nanjing, in 2007. From June 2007 to October 2009, he was a Research Fellow with the Adastral Park Research Campus, University College London, London, U.K. He is currently with the Faculty of the National Mobile Communications Research Laboratory, Southeast University. His research interests include space time wireless communications, random matrix theory, and information theory. He serves as an Associate Editor for the IEEE Transactions on Wireless Communications, IEEE Communications Letters, and IET Communications. He and his coauthors have been awarded the 2011 IEEE Communications Society Stephen O. Rice Prize Paper Award in the field of communication theory and the 2010 Young Author Best Paper Award by IEEE Signal Processing Society.

Quan Yu received his B.S. degree in radio physics from Nanjing University, China, in 1986, his M.S. degree in radio wave propagation from Xidian University, China, in 1988, and his Ph.D. degree in fiber optics from the University of Limoges, France, in 1992. He is currently a Research Professor at Peng Cheng Laboratory. His main areas of research interest are the architecture of wireless networks and cognitive radio. He is an Academician of the Chinese Academy of Engineering (CAE) and the founding Editor-in-Chief of the Journal of Communications and Information Networks (JCIN).